

Behavior of self supported transmission line towers under stationary downburst loading

Mohamed M. Darwish¹ and Ashraf A. El Damatty*²

¹March Consulting Associates Incorporation Saskatoon, Saskatchewan, Canada, S7K 0B8

²Department of Civil and Environmental Engineering, The University of Western Ontario London, Ontario, Canada, N6A 5B9

(Received August 27, 2010, Accepted May 17, 2011)

Abstract. During the past decade, many electrical transmission tower structures have failed during downburst events. This study is a part of a research program aimed to understand the behaviour of transmission lines under such localized wind events. The present study focuses on assessing the behaviour of self supported transmission line towers under downburst loading. A parametric study is performed to determine the critical downburst configurations causing maximum axial forces for various members of a tower. The sensitivity of the internal forces developing in the tower's members to changes in the downburst size and location was studied. The structural behaviour associated with the critical downburst configurations is described and compared to the behaviour under 'normal' wind loads.

Keywords: downburst; transmission lines; finite element; self-supported transmission towers.

1. Introduction

Transmission towers are essential components in an electrical system. A major cause of power outages is the failure of the towers during severe natural disasters. These costly failures have been often attributed to high localized wind events, in the form of tornadoes and downbursts (Manitoba Hydro 1999). Despite these facts, the design codes of transmission towers have typically considered only wind loads associated with large-scale synoptic events, such as hurricanes and typhoons. High intensity winds (HIW), resulting from downbursts, originate from thunderstorms. A downburst was defined by Fujita (1990) as "a strong downdraft that induces an outburst of damaging winds on or near the ground". The boundary layer wind velocity profile of large-scale wind events is typically different from that of a downburst. As such, downbursts can produce different loading and, consequently, different collapse modes, as shown by Kim *et al.* (2007) for the case of tall buildings.

In general, the structural system of electrical transmission towers can be categorized into two types: (a) self-supporting towers, and (b) guyed towers. Guyed towers rely on attached guys, which are anchored to the ground, to transfer some of the lateral loads imposed on the tower. Under lateral loads, guyed towers behave as simple beams with overhanging cantilevers. The towers are simply supported at their bases, while the guys function as flexible supports. On the other hand, self-supporting towers carry and transfer loads only through its members. Under lateral loads, a self-

* Corresponding Author, Professor, E-mail: damatty@uwo.ca

supporting tower behaves similar to a cantilever with the tower base fixed to the ground.

Savory *et al.* (2001) modeled the wind velocity time-histories of transient tornado and microburst events and applied their resulting loads on a lattice self-supported transmission tower. The dynamic analysis performed for the two HIW events predicted a shear failure due to the tornado similar to that observed in the field. However, the microburst did not cause a failure due to its lower intensity (in comparison to the tornado).

Kanak *et al.* (2007) studied a downburst event that occurred in south-western Slovakia in 2003. At least 18 electric self-supported transmission line towers were destroyed due to that downburst event. Seven of the transmission towers fell down in a 1.2 km line, where the transmission line was almost perpendicular to the track of the storm. The direction of the fallen towers and trees was almost uniform and parallel to the track of the thunderstorm. When observing the towers that failed during the event, it was found that the members in the middle third of the towers' height failed while the uppermost members and lowermost members remained straight. The firm that designed the transmission line reported that the structure could withstand a wind speed of 160 Km/hr (44.4 m/s). This suggested that the velocity acting on the transmission line was higher than 44.4 m/s. This high velocity causing failure (which could be the maximum velocity within the event) was appearing to be localized at the location of the failed towers (Kanak *et al.* 2007).

Hangan and Kim (2004 and 2007) developed and validated a computational fluid dynamic (CFD) model simulating the spatial and time variations of the time-varying mean component of the downburst velocity wind field. Shehata *et al.* (2005) developed a structural analysis numerical model capable of evaluating the response of transmission lines under the effect of downbursts. In this numerical model, the CFD data developed by Hangan and Kim (2004) was incorporated and scaled-up based on the relative values between the characteristics of a prototype downburst and those used in the CFD model. Shehata *et al.* (2005) structural analysis model was based on the finite element method, using three-dimensional linear frame elements to model tower members and two-dimensional non-linear curved frame elements to model conductors.

Shehata *et al.* (2005) reported a value of 0.58 s for the natural period of a 44 m high guyed transmission tower. The loading period of the mean velocity in the downburst model used in this study is greater than 20 s. This negates the need to perform a dynamic analysis, and consequently, Shehata *et al.* (2005) performed a quasi-static analysis.

Using this structural analysis model, Shehata and El Damatty (2007) conducted a parametric study by varying the jet diameter (D_j) and the location of the downburst center relative to the tower. A guyed transmission tower located in Manitoba, Canada, which collapsed in 1996 due to a downburst event, was used to perform this parametric study. The critical downburst parameters, in terms of the size of the event and its location relative to the tower, leading to maximum forces in the tower members, were identified. The study revealed that the critical downburst parameters vary based on the type and location of the members. Shehata and El Damatty (2008) extended their numerical scheme by including a failure model for the tower members, which was used to study the progressive collapse of the guyed tower that failed in Manitoba, Canada in 1996. An optimization routine was then implemented by Shehata *et al.* (2008) to predict the critical downburst parameters and the corresponding forces in an automated procedure.

In a previous study conducted by Darwish (2010), the effect of the translation velocity of the downburst on the behaviour of guyed transmission towers was assessed. In this study, the translation velocity was incorporated with the three critical downburst configurations that lead to potential failure of a tower. The first configuration was asymmetric with a projection angle $\theta = 30^\circ$, leading

to uneven distribution of forces on the conductor spans. In the second configuration, the load was symmetric with $\theta = 0^\circ$ such that the downburst flow field is perpendicular to the line. For the third configuration, the load was also symmetric with $\theta = 90^\circ$ and a downburst flow field parallel to the line. The study revealed that for the first case, the failure is triggered first when an assumption of zero translation velocity is made. In this case, the velocity profile results only from a stationary downburst. Such a configuration increases the variations of the velocity between adjacent spans of the conductors, leading to larger variations in the acting forces and, consequently, a larger unbalanced longitudinal force in the conductors, which is the major cause of failure. For the other two cases, the velocities triggering failure remained unchanged whether or not a translation velocity was included. In other words, the tower failed at the same radial velocity regardless of the contribution of the translation component into this velocity. In these two cases, the horizontal profile of the downburst velocity field resembles to a large extent the profile of large scale events and the spatially constant translation velocity does not alter this profile.

In view of the above findings, it can be concluded that there is no need to consider the translation velocity of the downburst and it is sufficient to conduct a parametric study through varying the location of the downburst in space by considering a large number of separate stationary events.

It should be mentioned that the above downburst studies have focused on guyed towers. The current study focuses on the behaviour of self-supported transmission towers under downbursts. The study is conducted numerically using the same model developed by Shehata *et al.* (2005). A brief description of this numerical model is first introduced. An extensive parametric study is conducted to assess the structural behaviour of a self-supported tower, while varying the downburst parameters, which are defined by the diameter of the downburst jet and the location of the centre of the downburst relative to the centre of the tower. The results of this parametric study are used to assess the variations of the internal forces in various tower's members with the downburst parameters. They are also used to identify the critical downburst configurations that lead to maximum internal forces in various members of the tower. The internal forces associated with the critical downburst configurations are compared to those corresponding to normal wind loads that are typically used in the design. Finally, the structural behaviour of the self-supported tower under such critical downburst configurations is described.

2. Description of numerical model

As mentioned above, the current study was conducted using the numerical model developed by Shehata *et al.* (2005). The wind field for downbursts adopted in this model is based on the Computational Fluid Dynamic (CFD) simulation conducted by Hangan and Kim (2004, 2007). The variations of the wind field, with time and space, for a small-scale downburst jet having a specific diameter and a certain downward velocity, were determined from the CFD simulation. The downburst velocity field has two components; a radial horizontal component and an axial vertical component. A procedure to scale-up this wind field and to estimate the wind forces acting on the tower and the conductors due to a full-scale downburst was provided by Shehata *et al.* (2005). The magnitude and direction of these forces depend on a number of parameters, which are referred to as "the downburst configurations". These parameters are: (a) the jet velocity (V_j), (b) the jet diameter (D_j), (c) the location of the centre of the downburst relative to centre of the tower, which is defined by the polar coordinates r and q .

Shehata *et al.* (2005) found that the radial (horizontal) component of the downburst velocity is higher in magnitude than the axial (vertical) component. Fig. 1 shows the variation of the radial velocity component (normalized by the jet velocity) with the height for different radial locations. It could be noticed that the largest values of the radial velocity occurs at a ratio r/D_j of 1.2; this maximum velocity is 10% more than the jet velocity and is nearly constant for heights ranging between 35 m and 75 m.

Two types of elements were used in Shehata's numerical model. The tower members were modeled using two-noded linear three-dimensional frame elements having three translational and three rotational degrees of freedom per node. The conductors were modelled using an assembly of two-dimensional nonlinear curved consistent frame elements (Gerges and El Damatty 2002). This nonlinear model took into consideration various nonlinear aspects that affect the behaviour of flexible cables, including the effects of sagging, pre-tensioning forces, and large deformations. After assuming a specific downburst configuration and evaluating the corresponding downburst forces, the numerical model started by conducting two independent quasi-static time history analyses for each conductor (one analysis for each velocity component). This set of analyses included modeling three conductor spans from each side of the tower of interest. It was shown by Shehata *et al.* (2005) that this number of spans is sufficient to predict the forces transferred from the conductors to the tower. In these analyses, the conductors are supported by nonlinear springs at their connections with the towers. The stiffness of these springs simulated the combined rigidity of the towers and the insulators used to connect the towers cross arms to the conductors. Time history variations for the three components of the reaction force, transferred from the conductors to the tower of interest, were determined from this set of analyses. This was followed by a linear time history quasi-static analysis for the tower under the combined effects of the downburst wind forces acting on the tower members and the conductors' reaction forces predicted by the first set of analyses. Time history variations for the tower members' internal forces were determined from this set of analyses.

For each member, the absolute maximum internal force determined within the entire time history of the analysis was detected. A parametric study was conducted by repeating the analyses many times through varying the downburst parameters (D_j , r and θ). The jet velocity (V_j) was usually assumed to have a fixed value in this parametric study. The absolute maximum force in each member of the tower obtained from the entire parametric study could be then determined. The critical downburst configurations (D_j , r and θ) corresponding to this maximum force could also be

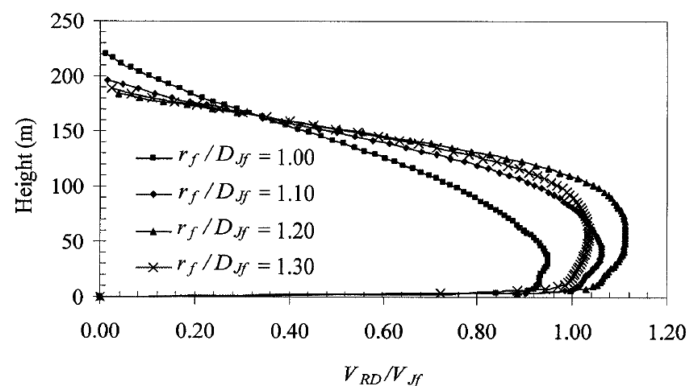


Fig. 1 Vertical profile of the radial outflow wind associated with a downburst. (Shehata *et al.* 2005)

identified. In general, the tower members can have different critical downburst configurations. Usually, a certain number of critical downburst configurations exist for a tower. These downburst configurations need to be considered when attempting to design the tower to resist downbursts.

In the current study, a self-supported transmission tower, belonging to Manitoba Hydro and labelled as A-501-0, was considered for downburst analysis. The system of global axes used in the finite element analysis of the entire transmission line/tower system is shown in Fig. 2, where the Y -axis coincides with the transmission line, the Z -axis is the vertical direction, and the X -axis is perpendicular to the transmission line.

The geometry and dimensions of this tower are shown in Fig. 3. As shown in Fig. 3, the considered tower carries three conductors and two ground wires. Two conductors are connected to the tower (one on each side) through insulators at a height of 35.11 m, while the third conductor is connected to two insulators at two separate points, both at a height of 44.51 m. The conductors span and sag are 420 m and 15 m, respectively. The initial pretension force applied to the conductors has a value of 48,180 N. Modeling of the tower and conductors and the sequence of analysis follow the procedure established by Shehata *et al.* (2005).

3. Parametric study of a self supported tower

As shown in Fig. 3, the tower A-501-0 is divided into six zones. The uppermost two zones carry the conductors and ground wires, while the lowermost four zones constitute the major part of the tower body.

The parametric study focuses on evaluating the effects of changing the downburst diameter (D_j), the downburst location described by the distance to diameter ratio (r/D_j), and the projection angle (θ), on the internal forces of the tower's members. Results of the parametric study were used to: (a) identify the maximum internal forces in the members and the critical downburst parameters

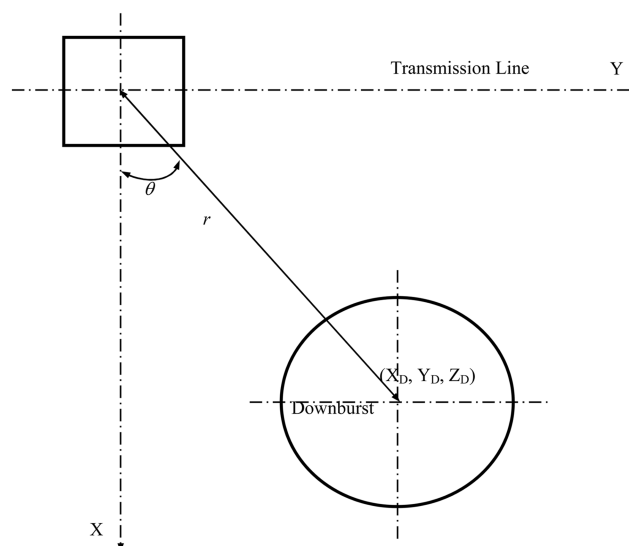


Fig. 2 Horizontal projection of transmission tower and downburst parameters. (Shehata *et al.* 2005)

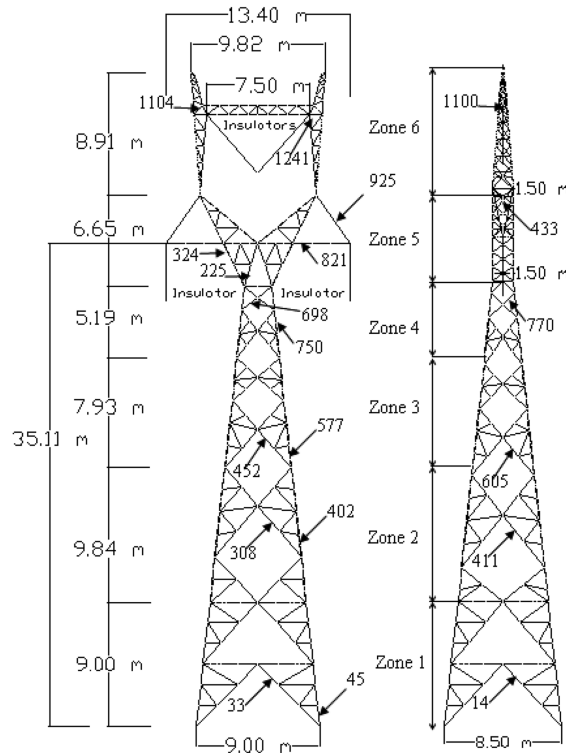


Fig. 3 Geometry of MH tower type A-501

corresponding to those forces, (b) assess and plot the variations of the member internal forces with the downburst parameters.

A fixed value for the jet velocity (V_j) of 40 m/s was assumed in all analyses conducted in this parametric study. The range of parameters considered in the study was as follows:

- $D_j = 500$ m, 1000 m and 2000 m, respectively
- r/D_j from 0 to 2.2 using an increment of 0.2
- θ from 0° and 90° using an increment of 15°

The results are presented for some selected members of the tower. The locations of the selected members are shown in Fig. 3. For Zones 1 to 4, which constitute the main body of the tower, one chord and two diagonal members are selected for each zone. The two diagonal members are located in two different planes; parallel and perpendicular to the line direction, and are labelled as diagonal (I) and diagonal (II), respectively. A similar selection is made for zone 6. In addition to the above three types of members, the forces in one upper chord member and one bottom chord member are reported in the conductor cross arm area (zone 5).

3.1 Maximum member forces and critical downburst parameters

The maximum axial forces in the selected members resulting from the parametric study are reported in Table 1. The results are presented with and without the inclusion of the self weight of the structure. The critical downburst configurations corresponding to the maximum forces are

Table 1. Parametric study for the manitoba hydro tower type A-501-0

Zone	El.	Type	Downburst load				ASCE	
			D_j (m)	r/D_j	θ	Force including own weight (KN)	Force excluding own weight (KN)	Force (KN)
1	45	Chord	500	1.4	15	329.1	313.2	302.5
	14	Diagonal (I)	500	1.2	90	7.1	7.7	7.1
	33	Diagonal (II)	500	1.2	0	9.9	10.0	12.2
2	402	Chord	500	1.4	15	348.0	334.7	325.8
	411	Diagonal (I)	500	1.2	90	4.7	4.4	4.0
	308	Diagonal (II)	500	1.2	0	14.4	18.8	14.0
3	577	Chord	500	1.4	15	337.6	325.5	319.9
	605	Diagonal (I)	500	1.4	30	6.6	6.2	1.8
	452	Diagonal (II)	500	1.4	15	10.3	4.9	3.9
4	750	Chord	500	1.4	15	314.0	302.8	300.8
	770	Diagonal (I)	1000	1.2	0	-5.5	4.3	4.5
	698	Diagonal (II)	1000	1.2	0	27.8	46.0	50.2
5	324	Chord	1000	1.2	0	86.3	52.3	54.2
	433	Diagonal (I)	500	1.6	30	11.6	9.8	3.0
	225	Diagonal (II)	500	1.4	15	170.2	136.9	139.5
6	925	U. Chord	500	1.6	30	46.2	33.4	0.7
	821	L. Chord	500	1.8	60	10.0	2.5	3.3
	1241	Chord	1000	1.2	0	73.1	72.0	78.7
6	1100	Diagonal (I)	500	1.8	60	7.2	1.6	1.6
	1104	Diagonal (II)	1000	1.2	0	21.9	23.4	25.8

reported for each member. In addition, a set of external forces simulating normal wind loads were calculated based on the ASCE 74 (2010) equations using a reference velocity of 40 m/s. The tower was analyzed under this set of forces and the axial loads developing in the selected members are provided in Table 1 for purpose of comparison. The following observations can be made from the results provided in Table 1:

- For the chord members of zones 5 and 6, the maximum forces correspond to $D_j = 1000$ m, $r/D_j = 1.2$ and $\theta = 0^\circ$. At this location, the radial velocity of the downburst becomes perpendicular to the line. This leads to maximum values for the conductor transverse reaction. Probably, this is why this configuration is the critical one with respect to these members. No unbalanced forces act on the conductors under this configuration and, consequently, no net longitudinal reaction acts on the tower. The r/D_j value of 1.2 leads to the maximum values for the vertical profile of the radial velocities. This could explain why this ratio turns out to be critical in this case. The relatively large value for the jet diameter $D_j = 1000$ m allows a larger length of the conductors to be subjected to large velocity values.

- For chord members of zones 1 to 4, the critical downburst parameters are $D_j = 500$ m, $r/D_j = 1.4$

and $\theta = 15^\circ$. The critical angle is still close to the $\theta = 0^\circ$ leading to large values for the transverse reactions. In addition, this small offset of the downburst location leads to a longitudinal conductor reaction, which results in a transverse overturning moment resisted by the chord members.

- Most of the diagonal (II) (perpendicular to the line) members have a critical angle $\theta = 0^\circ$. This downburst location leads to maximum values for the external forces acting in the direction perpendicular to the line.

- For diagonal (I) members, one would expect that the maximum axial forces occurs at $\theta = 90^\circ$. This happens for members 14 and 411 located in zones 1 and 2. In other zones, the critical angle varies between 0° to 60° . This can be interpreted by the following two reasons: (a) since the four legs of the tower are inclined, the plane at which diagonal (I) members exist is not totally parallel to the line. As such, the external forces perpendicular to the line will have a component in this plane, (b) the projected area perpendicular to the line is significantly larger than the projected area parallel to the line. This is particularly true at the top portion of the tower, where the critical angles deviate from the 90° value.

- The upper and lower chord members of zone 5 have intermediate critical angles of $\theta = 30^\circ$ and 60° , respectively. This is due to the longitudinal conductor reaction associated with these unbalanced load cases. Large internal forces develop due to the out-of-plane bending resulting from this longitudinal force.

- With the exception of the upper chord of the cross arm, the internal forces resulting from both the ASCE and the downburst analyses have close values. More details about this variation are discussed in Section 4.

3.2 Sensitivity of the tower member forces to changing downburst configuration

The results of the parametric study were used to assess the sensitivity of the tower members internal forces with the three downburst parameters; D_j , r/D_j , and θ . The variations of the axial forces for some selected members, as well as the conductor reactions, with these parameters are provided in Figs. 4 to 8. The following observations can be made from these Figs:

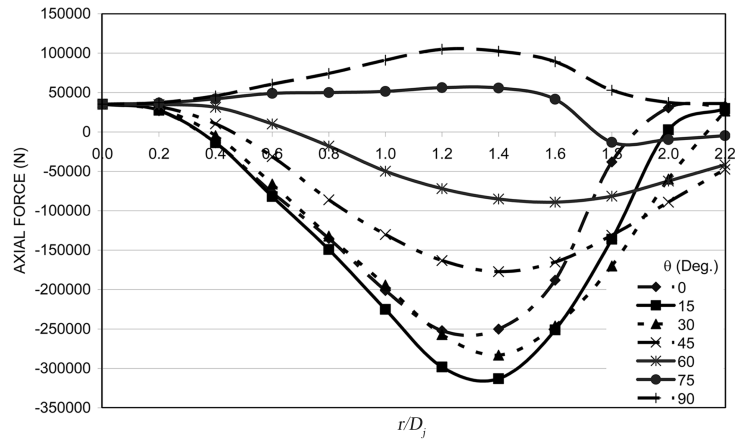
- The variation in r/D_j has a significant effect on the values of the axial forces for all members of the tower.

- For most of the members, the axial forces increase with the decrease in diameter and the largest forces occur for a jet diameter equal to 500 m (which was the lower bound diameter used in the study).

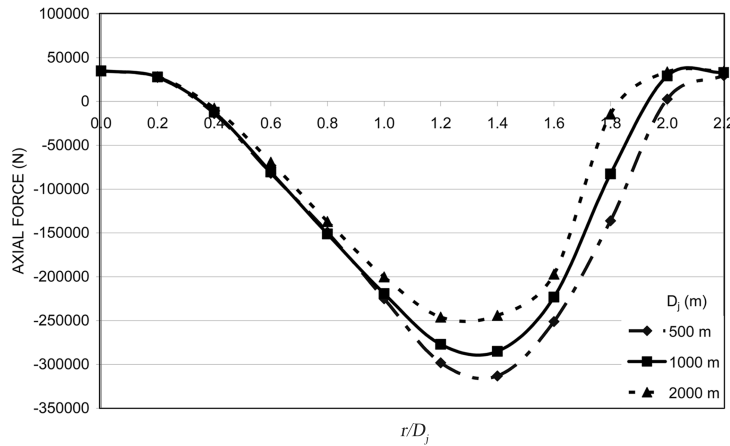
- For members with a critical jet diameter of 1000 m, the differences between the two curves of 500 m and 1000 m diameters are minute, as shown in Figs 4(b) and 6. It can be concluded from Figs. 4 to 7 that the effect of varying D_j is less significant than the effects of varying r/D_j and θ .

- Fig. 4(a) shows that for the chord member located in Zone 1, the difference between the peak values of the two curves representing angles of 15° and 30° is approximately 10% with a maximum value occurring at 15° . Fig. 5 shows that, for the upper chord cross-arm member located in Zone 5, the difference between the peak values associated with angles of 15° and 30° is more than 10% with an absolute maximum value occurring at 30° . On the other hand for zone 6, the absolute maximum value occurs at an angle of 0° , as shown in Fig. 7.

- As shown in Fig. 8, a maximum value for the conductor longitudinal reaction of 12,000 N occurs at two values of r/D_j , which are 1.6 and 1.8. They correspond to two different critical angles of 30° and 45° , respectively. It can be also noticed that the difference between this absolute



(a) Variation of the axial force with r/D_j and θ , for $D_j = 500$ m



(b) Variation of the axial force with r/D_j and D_j , for $\theta = 15^\circ$

Fig. 4 Variation of the axial force in member 45 (Zone 1) with the downburst parameters

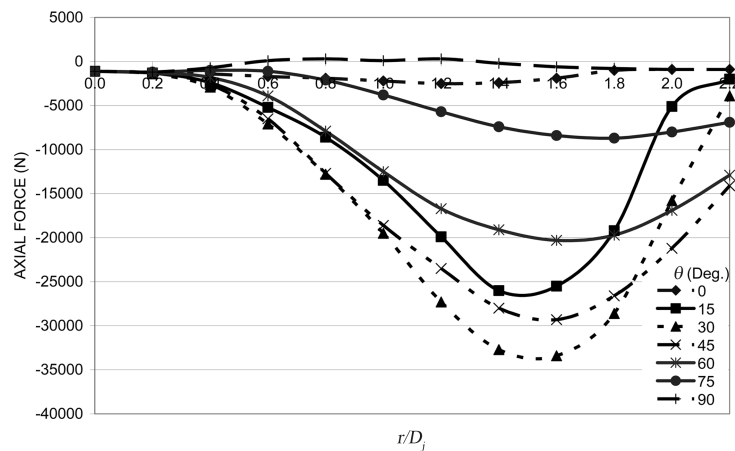


Fig. 5 Variation of the axial force in member 925 (Zone 5) with r/D_j and θ , for $D_j = 500$ m

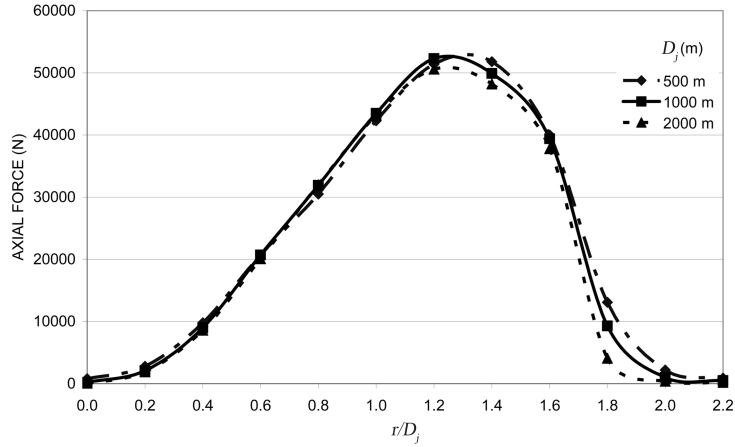


Fig. 6 Variation of the axial force in member 324 (Zone 5) with r/D_j and D_j , for $\theta = 0^\circ$

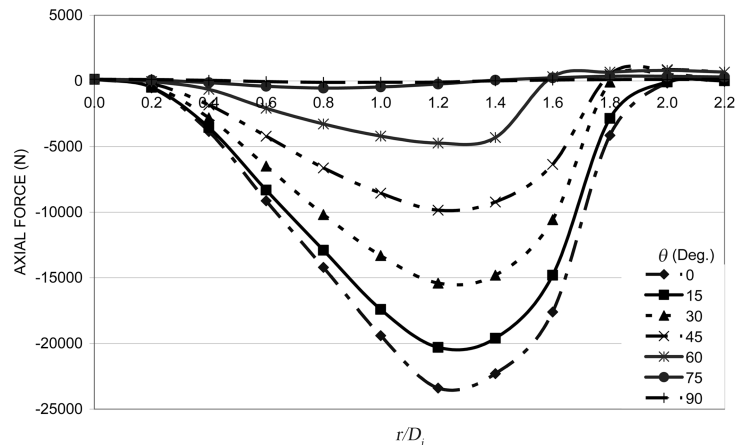


Fig. 7 Variation of the axial force in member 1104 (Zone 6) with r/D_j and θ , for $D_j = 1000$ m

maximum reaction and the value of 10,500 N, which is the peak reaction for both $\theta = 60^\circ$ and 15° , is not very large. Fig. 8(b) shows that a maximum value of 26,000 N for the transverse reaction occurs at an r/D_j of 1.2 and an angle of 0° which is expected as this load case is perfectly symmetric.

· The angle causing the second highest transverse reaction of 24,000 N is 15° . This value is only 8 % lower than the absolute maximum. This points out why the 15° angle causes the maximum axial forces in six of the twenty members presented in Table 1. This location of the downburst causes large reactions in both the transverse and the longitudinal directions. The biaxial moments resulting from this case lead to large axial forces in the chord members of zones 1, 2, 3 and 4 which are due to the fact that the chord members of the lower zones are the main mode of transmitting the straining actions resulting from the conductors and the ground wires forces to the ground. Such behaviour is different than that of guyed towers, in which the guys transmit these straining actions directly to the ground.

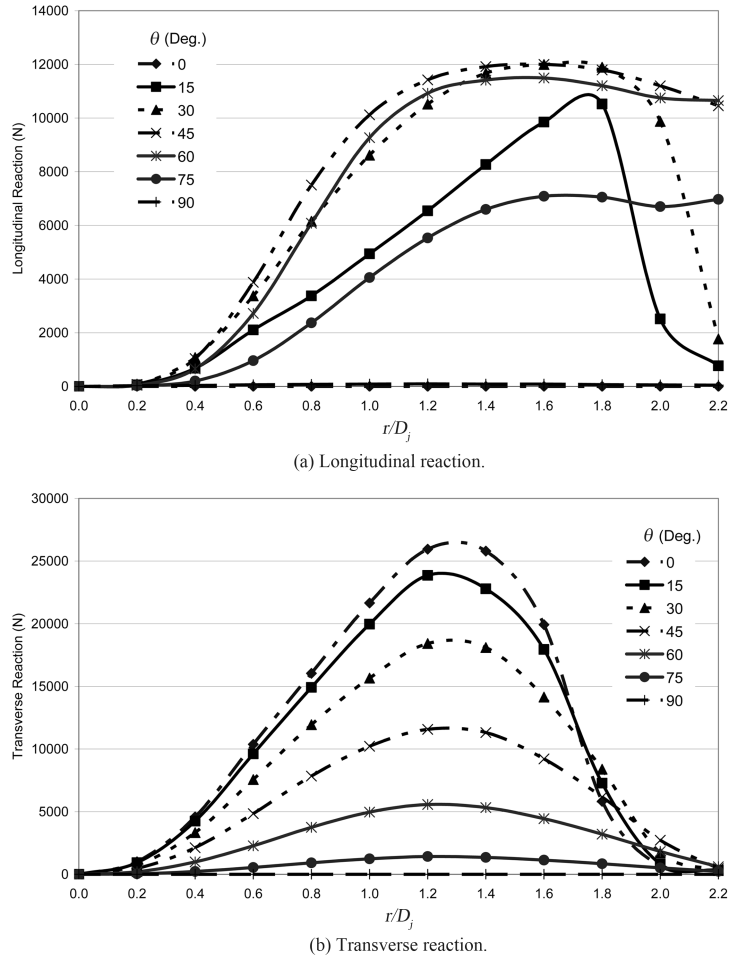


Fig. 8 Variation of the conductor reactions with r/D_j and θ , for $D_j = 500$ m

4. Behaviour of the self supported tower under downburst and normal wind loadings

The purpose of this section is to illustrate the behaviour of self supported transmission towers due to loading resulting from the critical downburst configurations and to compare it to the behaviour under normal wind loads. Four downburst configurations, which are shown to be critical according to the results provided in Table 1, are considered in this section.

4.1 Case I ($\theta = 0^\circ$)

The results provided in Table 1 suggest that two downburst configurations having an angle of 0° cause maximum forces in seven of the twenty members provided in that table. Both cases have the same value of 1.2 for the r/D_j ratio and both provide nearly the same vertical profile for the radial velocity. As shown in Table 1, the downburst having $D_j = 1000$ m, $r/D_j = 1.2$ and $\theta = 0^\circ$ leads

to maximum forces in the diagonal members (in both directions) in Zone 4, in the chord members of Zones 5 and 6, and in the diagonal members perpendicular to the transmission line in Zone 6. On the other hand, the downburst having $D_j = 500$ m, $r/D_j = 1.2$ and $\theta = 0^\circ$ leads to maximum forces in the diagonal members perpendicular to the transmission line in Zones 1 and 2. However, Figs. 4 to 7 show that the differences in results produced by downbursts having different jet diameters are minor. Therefore, when studying the behaviour of the considered self supported transmission tower, it is acceptable to focus only on its behaviour under one of these two cases. Since the case with a jet diameter of 1000 m is critical for four of the six members mentioned above, it is chosen to be studied in this section to represent the behaviour of this tower when it is subjected to a downburst with an angle of 0° .

A simulation for the tower as a vertical column unrestrained along its height and fixed at its base is shown in Fig. 9. The distributed loads, shown in Fig. 9(a), represent the external forces acting at various locations along the height of the tower due to a downburst having the above mentioned characteristics. In addition to that distributed load, the three concentrated forces shown represent the transverse reactions transferred from the two conductors at a height of 35.11 m; one conductor at a height of 44.51 m, and two ground wires at the top of the tower. Similar forces resulting from normal wind loads, calculated using ASCE No.74 guidelines (2010), are shown in Fig. 9(b).

A comparison between the downburst and the normal wind profiles indicates that the distributed forces acting on the tower are almost equal for both cases. On the other hand, the forces acting on the conductors due to normal wind loading exceed significantly those due to downburst loading. This could be attributed to the fact that the radial component of the velocity profile decreases when the ratio r/D_j exceeds 1.2. In the considered case, the relative distance r between the centers of the downburst and the tower satisfies a ratio r/D_j of 1.2. However as for the conductors, the effective value of r/D_j at different points will exceed 1.2 and, therefore, smaller forces act at these locations.

Fig. 10 shows the displacement profile and the variations of the overturning moment and shear force along the height of the equivalent beam due to both the downburst and normal wind loads, respectively. The large conductor forces associated with the normal wind load case lead to larger deflections and larger magnitudes for the overturning moments and shear forces along the height of the tower, which behaves as a cantilever.

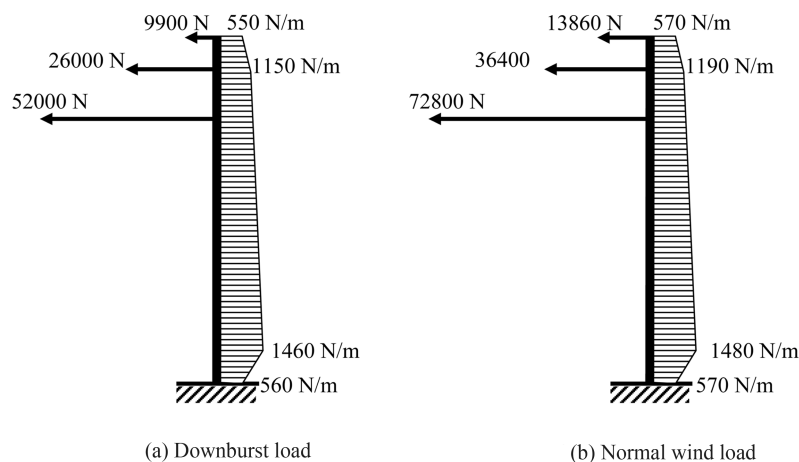


Fig. 9 Vertical profile of wind loading at a projection angle of 0°

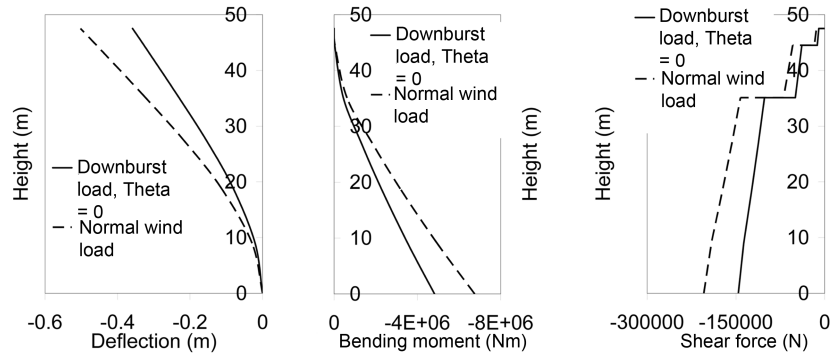


Fig. 10 Structural behaviour at a projection angle of 0°

4.2 Case II ($\theta = 15^\circ$)

The downburst configuration having $D_j = 500$ m, $r/D_j = 1.4$, $\theta = 15^\circ$ and $V_j = 40$ m/s is considered in this case. As shown in Table 1, this configuration leads to maximum forces in six of the twenty members provided in that table. These members are the chord members of zones 1, 2, 3 and 4, and the diagonal members perpendicular to the transmission line in zones 3 and 5. The uniqueness of this downburst configuration is that it causes, simultaneously, large longitudinal and transverse reactions in the conductors and ground wires, which are transmitted to the tower. Hence, the behaviour of the tower under this load case is studied twice; once in the transverse plane, and the other in the longitudinal plane.

A simulation similar to that used for the 1st case is shown in Fig. 11. The distributed loads, shown in Fig. 11(a), represent the transverse component of the loads acting at various locations along the height of the tower due to a downburst having the above mentioned characteristics. In addition to that distributed load, the three concentrated forces shown in the same figure represent the transverse reactions transferred from the two conductors at a height of 35.11 m; one conductor at a height of 44.51 m, and two ground wires at the top of the tower. Similar forces resulting from normal wind loads, calculated using ASCE No.74 guidelines (2010), are shown in Fig. 11(b). Similar to the first case, the transverse conductors' reactions due to normal wind load exceed those due to downburst loading.

On the other hand, the distributed loads shown in Fig. 11(c) represent the longitudinal component of the loads acting at various locations along the height of the tower due to a downburst having the above mentioned characteristics. In addition to that distributed load, the three concentrated forces shown in the same figure represent the longitudinal reactions transferred from the conductors ground wires to the tower. Similar forces resulting from normal wind loads calculated using ASCE No.74 guidelines (2010) are shown in Fig. 11(d). While no longitudinal reactions are added to the distributed normal wind load as shown in Fig. 11(d), significantly large longitudinal forces are transferred from the transmission line to the tower in the case of downburst loading shown in Fig. 11(c).

Fig. 12(a) shows the transverse components of the displacement profile and the variations of the overturning moment and shear force in the transverse plane along the height of the equivalent beam due to both the downburst and normal wind loads, respectively. It could be noticed that the straining actions experienced in the transverse plane are very similar to those experienced in the first case. Fig. 12(b) shows the longitudinal components of the displacement profile and the variations of the

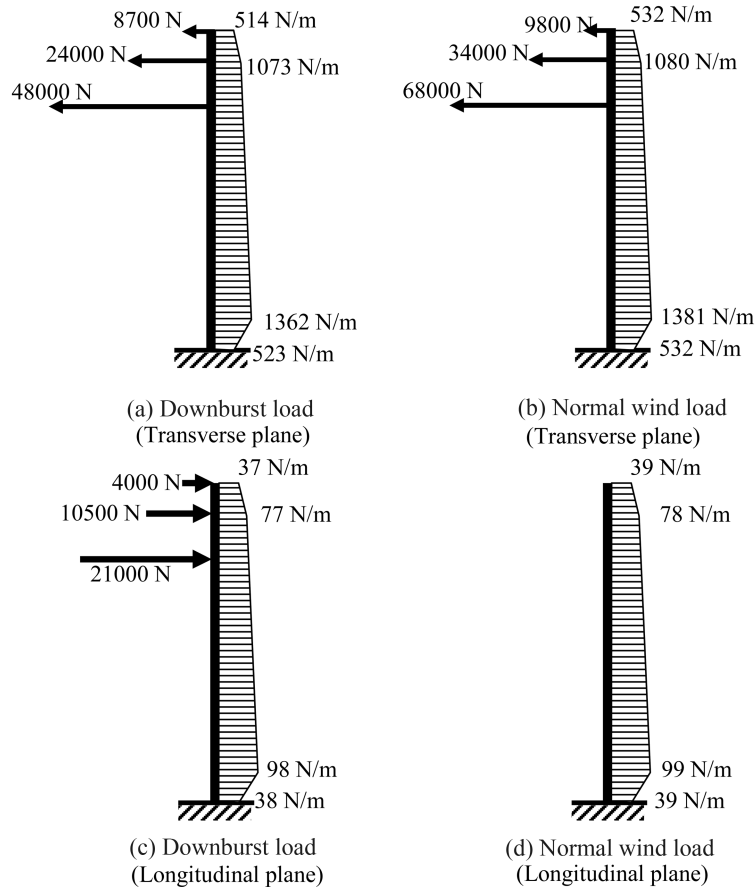


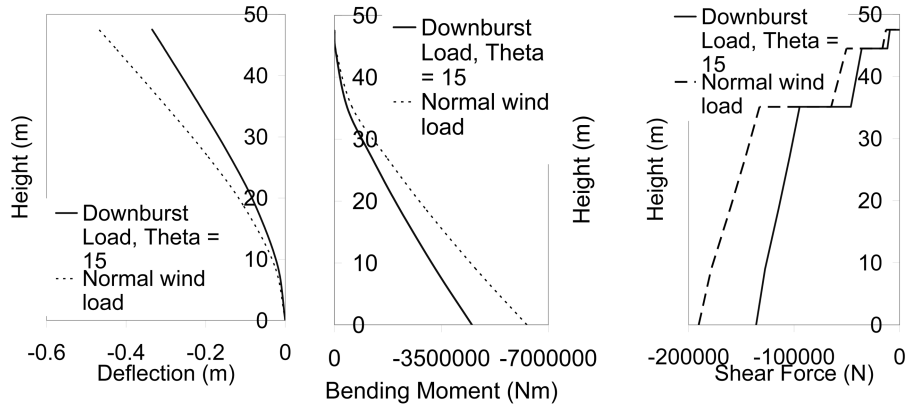
Fig. 11 Vertical profile of wind loading at a projection angle of 15°

bending moment and shear force in the longitudinal plane along the height of the equivalent beam due to both the downburst and normal wind loads, respectively.

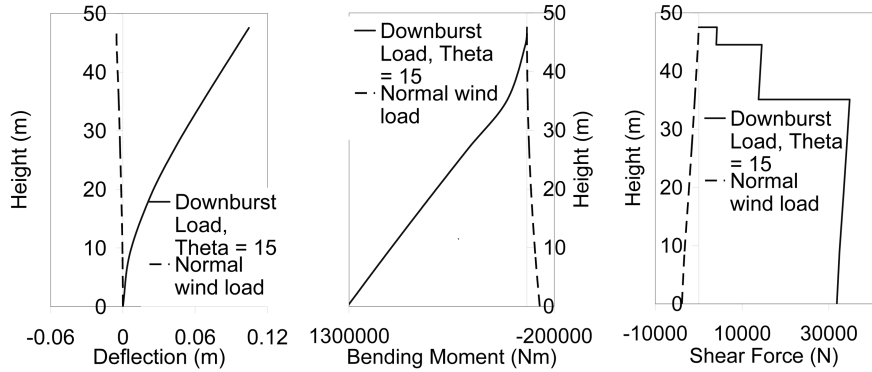
The large longitudinal forces associated with the downburst load lead to larger deflections and larger magnitudes of the bending moments and shear forces along the height of the tower. This points out why the chord members in Zones 1, 2, 3 and 4 experience high axial forces under this downburst load case, as these members resist moments resulting from both the longitudinal and transverse reactions.

4.3 Case III ($\theta = 30^\circ$)

The downburst configuration having $D_j = 500$ m, $r/D_j = 1.6$, $\theta = 30^\circ$ and $V_j = 40$ m/s is considered in this case. As shown in Table 1, this configuration leads to maximum forces in the upper chord member and in a diagonal member of the cross-arm zone (Zone 5). The uniqueness in this configuration is that it puts these members into compression while these members are designed to carry mainly tensile forces under the combined effects of normal wind load and the conductor self weight.



(a) Behavior of the tower in the transverse direction.



(b) Behaviour of the tower in the longitudinal direction.

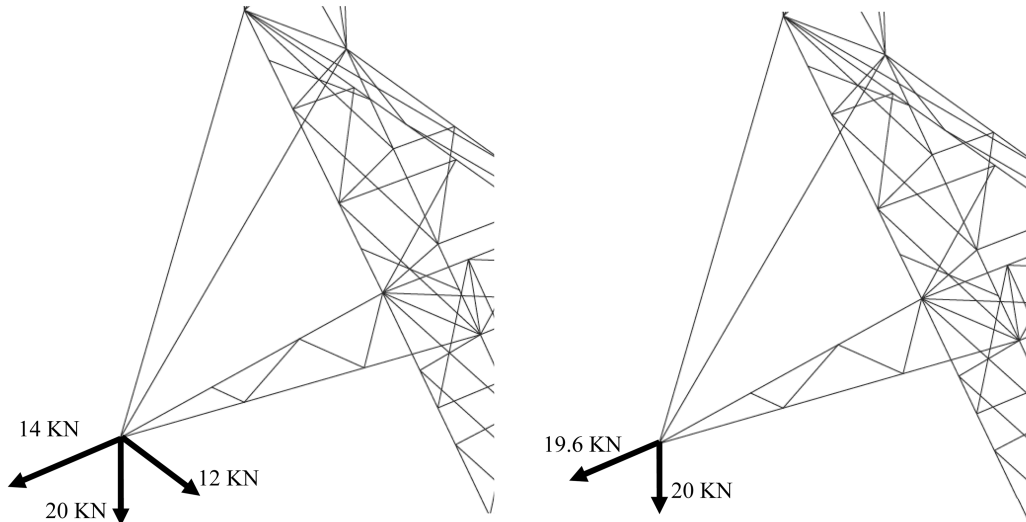
Fig. 12 Structural behaviour at a projection angle of 15°

This can be explained in view of the sketches provided in Fig. 13. The main difference between the forces shown in Fig. 13(a) for the case of downburst loading, having the described configuration, and the normal wind load, shown in Fig. 13(a), is the presence of the large longitudinal reaction acting at the tip of the cross-arm. This longitudinal reaction causes a significant out-of-plane bending on the cross arm which is resisted by equal tension and compression forces at the opposite faces of the cross arm. The upper chord member, which has an unsupported length of 4.37 m, might not be adequate to resist the acting compression force.

4.4 Case IV ($\theta = 90^\circ$)

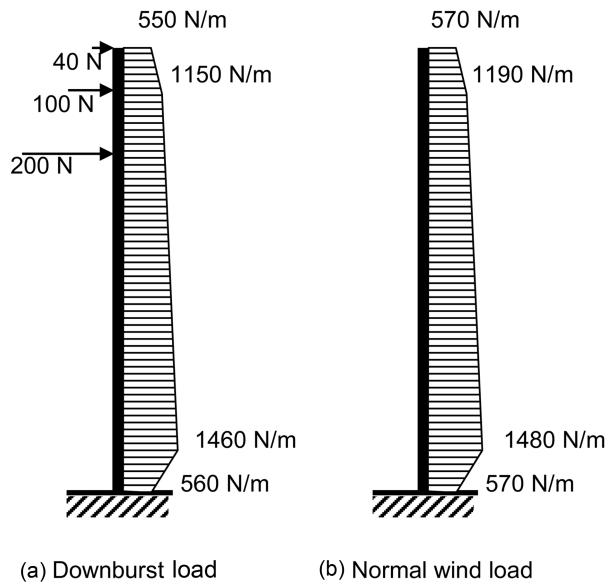
The results provided in Table 1 suggest that a downburst configuration having an angle of 0°, a ratio r/D_j of 1.2 and a jet diameter of 500 m causes maximum forces in the diagonal members perpendicular to the transmission line in the lowermost two zones.

The comparison between the forces associated with this downburst and the normal wind case shown in Fig. 14 indicates that the forces acting on the tower body are almost equal for both cases.



(a) Downburst load in addition to the conductor self weight. (b) Normal wind load in addition to the conductor self weight.

Fig. 13 Forces transferred from conductors under different wind loads at a projection angle of 30°



(a) Downburst load (b) Normal wind load

Fig. 14 Vertical profile of wind loading at a projection angle of 90°

On the other hand, no forces act on the conductors due to normal wind loading in comparison to those due to downburst loading. However, this does not cause a major difference in the structural response as the magnitudes of the longitudinal reactions in this case are small.

Fig. 15 shows the displacement profile and the variations of the bending moment and shear force along the height of the equivalent beam due to both the downburst and normal wind loads, respectively. The absence of conductor forces in the case of normal wind load leads to slightly

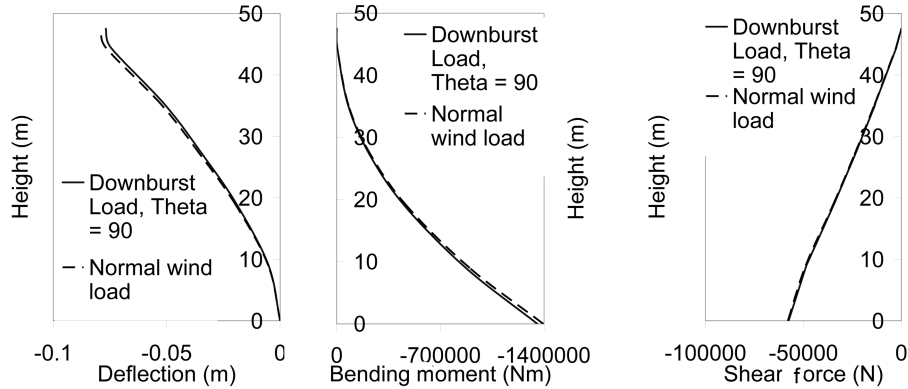


Fig. 15 Structural behaviour at a projection angle of 90°

smaller deflections (4% difference), and slightly smaller magnitudes (4% difference) of the bending moments and shear forces along the height of the tower.

5. Conclusions

This paper studies the behaviour of a self-supported transmission tower under downburst loading. A parametric study to determine the critical downburst configurations causing maximum axial forces for various members of the tower is performed. The sensitivity of the internal forces developing in the tower’s members to changes in the downburst size and location is studied. The general behaviour of the transmission tower due to each of the critical downburst load cases is described.

Based on the findings of this study, the following conclusions can be drawn:

1. Changing the location of the downburst (r/D_j and θ) has a stronger effect on the value of the axial force in all tower members when compared to the downburst size (D_j) which has a minor effect.
2. Due to the higher radial velocities for r/D_j of 1.2 and 1.4, the downbursts locations corresponding to these ratios cause critical load cases for the first four zones. Larger critical ratios occur for some members in the uppermost two zones.
3. The downbursts having $r/D_j = 1.2$ and $\theta = 0^\circ$ lead to maximum forces in the diagonal members perpendicular to the transmission line in zones 1 and 2, the diagonal members (in both directions) in zone 4, the chord members of zones 5 and 6 and the diagonal members perpendicular to the transmission line in zone 6.
4. The downburst having $D_j = 500$ m, $r/D_j = 1.4$, $\theta = 15^\circ$ leads to maximum forces in the chord members of zones 1, 2, 3 and 4 and in the diagonal members perpendicular to the transmission line in zones 3 and 5. This is due to the large forces transferred simultaneously from the conductors and ground wires in both the longitudinal and transverse directions.
5. The downburst configuration having $D_j = 500$ m, $r/D_j = 1.6$, $\theta = 30^\circ$ leads to maximum forces in the upper chord member and a diagonal member in the cross-arm zone (zone 5). The members are subjected to compression axial forces under this configuration. These members have relatively large unsupported length and might not have been designed to resist compression under normal wind loads and own weight.

6. The typical design of the transmission line according to ASCE No. 74 (2010) could be considered sufficient to resist downburst winds at angles of 0° and 90° while for moderate angles (e.g., 15° and 30°) these design procedures are insufficient due to the large longitudinal reactions occurring in these cases.

References

- American Society of Civil Engineers (2010), *Guidelines for electrical transmission line structural Loading*, ASCE Manuals and Reports on Engineering Practice, No. 74, N.Y.
- Darwish, M.(2010), *Characteristics and design of downburst loaded transmission lines*, PhD Thesis, University of Western Ontario, London, Ontario, Canada.
- Fujita, T.T. (1990), "Downbursts: meteorological features and wind field characteristics", *J. Wind Eng. Ind. Aerod.*, **36**(1), 75-86.
- Gerges, R.R. and El Damatty, A.A. (2002), "Large displacement analysis of curved beams", *Proceedings of CSCE Conference*, Montreal, QC, Canada.
- Hangan, H. and Kim, J.D. (2004), "Numerical simulation of downbursts", *Proceedings of the ASCE Structural Congress*, Nashville, Te, USA, June.
- Hangan, H. and Kim, J. (2007), "Numerical simulations of impinging jets with application to downbursts" *J. Wind Eng. Ind. Aerod.*, **95**(4), 279–298.
- Kanak, J., Benko, M., Simon, A. and Sokol, A. (2007), "Case study of the 9 May 2003 windstorm in south-western Slovakia", *Atmos. Res.*, **83**, 162-175.
- Kim, J.D., Hangan, H. and Ho, T.C.E. (2007), "Downburst versus boundary layer induced loads for tall buildings", *Wind Struct.*, **10**(5), 481-494.
- Koziey, B. and Mirza, F. (1994), "Consistent curved beam element", *Comput. Struct.*, **51**(6), 643-654.
- Manitoba Hydro Transmission and Civil Design Department (1999), "Bipole 1 & 2 HVDC transmission line wind storm failure on September 5, 1996review of emergency response, restoration and design of these lines", Manitoba Hydro, 98-L1/1-37010-06000, 54.
- Savory, E., Parke, G., Zeinoddini, M., Toy, N. and Disney, P. (2001), "Modelling of tornado and microburst-induced wind loading and failure of a lattice transmission tower", *Eng. Struct.*, **23**(4), 365-375.
- Shehata, A., El Damatty, A. and Savory, E. (2005), "Finite element modelling of transmission line under downburst wind loading", *Finite Elem. Anal. Des.*, **42**(1), 71-89.
- Shehata, A. and El Damatty, A. (2007), "Behaviour of guyed transmission line structures under downburst wind loading", *Wind Struct.*, **10**(3), 249-268
- Shehata, A. and El Damatty, A. (2008), "Failure analysis of a transmission tower during a microburst", *Wind Struct.*, **11**(3), 193-208
- Shehata, A., Nassef, A. and El Damatty, A. (2008), "A coupled finite element-optimization technique to determine critical microburst parameters for transmission towers", *Finite Elem. Anal. Des.*, **45**(1), 1-12.